DETECTION OF DUST LOADED AIRMASS IN SEAWIFS IMAGERY: AN EMPIRICAL DUST INDEX IN COMPARISON WITH MODEL-PREDICTED DUST DISTRIBUTION OVER THE PACIFIC IN APRIL, 1998

H. FUKUSHIMA,[1] M. SCHMIDT,[2] B. J. SOHN,[3] M. TORATANI,[1] I. UNO [4]

[1] *School of High-Technology for Human Welfare, Tokai University, Numazu, 410-0395 Japan*
[2] *SeaWiFS Project, NASA Goddard Space Flight Center, 970.2, Greenbelt, MD 20771 U.S.A.*
[3] *Dept. Earth Sciences, Seoul National University, Seoul, 151-742 Korea*
[4] *Research Institute for Applied Mechanics, Kyushu University, Kasuga, Fukuoka, 816-8580 Japan*

ABSTRACT

The paper first proposes an empirical algorithm for detecting dust-loaded airmass observed by Sea Wide Field-of-view Scanner (SeaWiFS). The proposed dust index formula is based on the curvature of the spectral reflectance estimated from the SeaWiFS band 4 (510 nm band) through band 8 (865 nm band) data, assuming "clear ocean water" reflectance. Evaluation of the algorithm is made over several typical Asian dust images including the ones over the Pacific in April, 1998, when a major dust event was reported. The study analyzes the performance and the characteristics of the algorithm by comparing the satellite-derived dust index images with contemporaneous columnar concentration of dust particles predicted by a numerical dust transport model. The comparison reveals several small-scale differences although their dust distribution patterns show good agreement generally.

INTRODUCTION

Mineral dust-rich aerosol, such as Saharan dust or Asian dust aerosol, is important in terms of its effect on radiation budget as well as its role as a source of micro-nutrient in the oceanic phytoplankton ecosystem. Mineral dust aerosol is considered to be absorptive and hence it affects the correction of the atmospheric effect in ocean color remote sensing.

There have been several works regarding satellite observation of dust aerosol. Herman *et al.* (1997) developed TOMS aerosol index to detect absorptive aerosol based on UV observation bands.

Moulin *et al.* (1997a and 1997b) proposed a method for evaluating the dust optical thickness and dust density using Meteosat. Fukushima and Toratani (1997) developed an algorithm for Nimbus-7/Coastal Zone Color Scanner to detect Asian dust aerosol and correct its effect on phytoplankton pigment estimate.

In this paper, we propose a preliminary dust aerosol detection algorithm for Sea Wide Field-of-View Scanner (SeaWiFS), whose primary purpose is to conduct global observation of phytoplankton pigment concentration. The instrument has 8 observation bands centered at 412, 443, 490, 510, 555, 670, 765, and 865 nm, with the band width of 20 nm for all the visible bands and 40 nm for 765 and 865 nm bands. A unique feature of SeaWiFS is that all the bands have bilinear input-output characteristic that allows the instrument to observe cloud-like bright targets without saturation.

The dust detection scheme proposed in the paper puts its base on estimated aerosol reflectance over 5 SeaWiFS bands, 510 through 865 bands namely, to detect spectral curvature in the aerosol reflectance. A performance test is conducted against several SeaWiFS images of April, 1998 over the East Asian waters as well as the whole pacific. The satellite-derived dust aerosol index images are also compared to the average column dust concentration predicted by a numerical dust transport model.

DEFINITION OF DUST INDEX

Radiative transfer model

We assume that the satellite reflectance $\rho_T(\lambda)$ is expressed as follows.

$$\rho_T(\lambda) = \rho_M(\lambda) + \rho_A(\lambda) + t(\lambda)t_0(\lambda)\rho_W(\lambda) \quad (1)$$

where λ is wavelength, ρ_M is the Rayleigh reflectance when the atmosphere consists of gas molecules only, and ρ_A is the reflectance of the aerosol, including the multiple scattering between aerosol particles and gas molecules. $\rho_W(\lambda)$ is the reflectance of water body defined as

$$\rho_W(\lambda) = \frac{\pi L_w(\lambda)}{E_s(\lambda)} \quad (2)$$

where $L_W(\lambda)$ is the water-leaving radiance and $E_S(\lambda)$ is the downward irradiance just above the sea-surface. t is the diffuse transmittance between spacecraft and sea surface, while t_0 is the diffuse transmittance between the sun and sea surface. We assume that (non-absorptive) aerosol does not have much influence on the transmittances, and hence, they are defined to be

$$t(\lambda,\theta) = \exp(-0.5\tau_M / \cos\theta), \quad (3)$$

and

$$t(\lambda,\theta_0) = \exp(-0.5\tau_M / \cos\theta_0). \quad (4)$$

where θ and θ_0 are the satellite and solar zenith angle, respectively.

For simplicity, we assume that all the components in (1) are the ones that would be observed in the absence of ozone and oxygen (for the 765 nm band only) absorption: In the actual data processing, we correct these absorption effects (Gordon, 1997).

Estimated aerosol reflectance

From (1), $\rho_A(\lambda)$ is expressed as

$$\rho_A(\lambda) = \rho_T(\lambda) - \rho_M(\lambda) - t(\lambda)t_0(\lambda)\rho_W(\lambda) \quad (5)$$

Since ρ_M, t and t_0 can be calculated, we can estimate ρ_A if we know ρ_W, which is variable in general. But if we concentrate our attention in observing aerosol over the open ocean where the water is clear enough, we can assume nominal clear water reflectance to retrieve estimates of ρ_A. To define the nominal values for clear water reflectance, we used the SeaBAM data set designed to develop and test the SeaWiFS biooptical algorithms. The data set consists of ship-measured in-water radiance data combined with the contemporaneous chlorophyll-a concentration data from about 1000 measurements (O'Reilly *et al.*, 1998: Maritorena *et al.*, SeaWiFS). From the data set, we extracted data with chlorophyll-a concentration of less than 0.1 mg/m^3. Table 1 shows the resulted clear water reflectance ρ_{W_CLEAR} for each visible band of SeaWiFS.

Table 1. Nominal clear water reflectance

Center wavelength [nm]	Mean water reflectance [ρ_{W_CLEAR}]
412	0.0364
443	0.0310
490	0.0210
510	0.0144
555	0.0047
670	0.000435

We should consider here how reliable these estimated ρ_A are since actual value of ρ_W varies depending on the in-situ (or pixel-wise) chlorophyll-a concentration. To investigate this, we partitioned the SeaBAM data set into several categories with respect to the chlorophyll-a concentration. Figure 1 shows mean water reflectances for the SeaBAM subsets, which have different ranges in the chlorophyll-a concentration of less than 0.07, 0.07-0.14, and 0.28-0.57 mg/m^3. We note that ρ_Ω values for the SeaWiFS bands of 490 nm or shorter wavelengths vary 1% or more over the range in the pigment concentration in question. This level of variability can be quite large since the range of aerosol reflectance we are interested in is below one to few per cent. Hence, we use estimated aerosol reflectance in the SeaWiFS band at 510 nm or longer. We also use the average of the estimated ρ_A values at 510 and 555 nm bands, hoping that it can cancel the variability in water reflectances in these bands, which covary but with negative correlation with the increase in chlorophyll-a concentration. Thus, we define $\rho_A(533)$ as

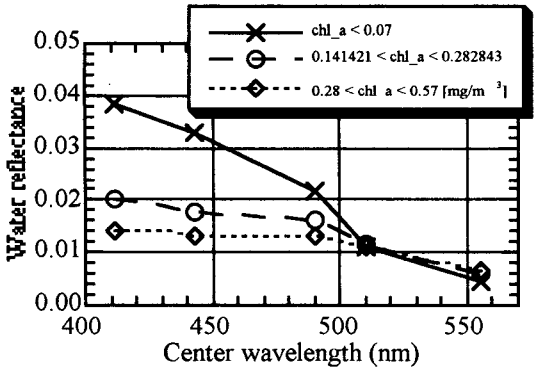

Figure 1. Mean spectral reflectance of water for the three classes of SeaBAM ship-measured data set. Each class contains about 100 to 200 data points with different ranges of chlorophyll-a concentration. Note that the larger variability of the reflectance in the shorter wavelength region.

$$\rho_A(533) = \frac{1}{2}\{\rho_A(510) + \rho_A(555)\} . \qquad (6)$$

Dust index formula

We first define the apparent Angstrom exponent $\alpha(\lambda_1, \lambda_2)$ as

$$\alpha(\lambda_1, \lambda_2) = -\frac{\log\{\rho_A(\lambda_1)/\rho_A(\lambda_2)\}}{\log(\lambda_1/\lambda_2)} . \qquad (7)$$

Using this, the empirical dust aerosol index *DI* is defined as

$$DI = \{\alpha(765,865) - \alpha(533,670)\} \times \rho_A(865) , \qquad (8)$$

where the value of ρ_A (865) is expressed in %.

The rationale for this formula is as follows. Due to the enhanced absorption effect in shorter wavelength region, we anticipate that the apparent Angstrom exponent α(533,670) is significantly lowered when the pixel is contaminated with dust aerosol. Observing the difference images between α (765,865) and α (533,670), we consider that the difference is significantly correlated with the aerosol composition (less difference when we expect maritime aerosol, larger difference when dust particles prevail). Hence we define the index as the difference of the two quasi-Angstrom exponent multiplied by the aerosol reflectance, the latter being used as the substitute for the total mass of the aerosol.

IMAGE ANALYSIS

SeaWiFS Scenes and data processing

We derived dust index imagery from several SeaWiFS GAC (Global Area Coverage, 4*4 km resolution) data that coveres Asian dust airmass observed in Japan and over the Pacific in April, 1998, when several large scale dust episodes were observed. We calculate the dust index value for every pixel unless it is over the land or ρ_A (865) for the pixel is higher than 10%. Note that this threshold is much higher than the cloud threshold of 3.5% used for the standard SeaWiFS Level-2 product.

Dust transport model simulation

For comparison purpose, we calculate the average columnar concentration of dust particles using the On-line Dust Transport Model (ONLT) developed by one of the authors (Uno, 1999). The simulation was made for the period of April 10 to 30, 1998 with grid spacing of about 120 km (for China-Korea-Japan area) or 200km (for the whole Pacific). Then, the results obtained for the time and space that match the SeaWiFS observations were selected and mapped into the same coordinates with the satellite-derived images. Since it takes SeaWiFS about 9 hours to observe the whole pacific, we made time-space composite of the model-predicted dust concentration images for the pacific, so that each of SeaWiFS imagery has the corresponding portion of predicted dust concentration in the composite.

DUST INDEX IMAGES AND PREDICTED DUST CONCENTRATION

Figure 2 (a) shows the SeaWiFS-derived dust index image of April 19, 1998 over Japan and the adjacent waters. The index value is generally higher in the area centering Japan, suggesting the presence of a dust air-mass. The black area within the satellite swath is "cloud" pixels, or the pixels with ρ_A(865) higher than 10%, which may also mean dense dust concentration.

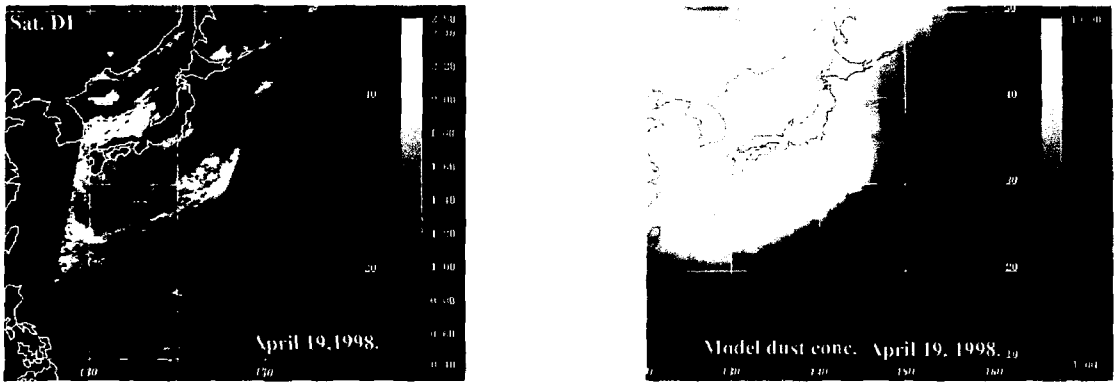

(a) (b)

Figure 2. SeaWiFS-derived dust index image (a) and corresponding model-predicted average column dust concentration (b) for April 19, 1998. The black area in the satellite swath is the pixels with the aerosol reflectance at 865 nm band higher than 10%. The unit of dust index is arbitrary whereas the model-predicted dust concentration value is expressed in micro g/m^3.

We compare this dust index with the contemporaneous average column dust concentration predicted by the numerical model (Fig. 2 (b)). Because of the cloud threshold, the satellite-derived image fails to reproduce the model-predicted dust distribution pattern, but the location of south most front of the dust airmass shows a good agreement. Another notable difference is that while the satellite image reveals very clear airmass along the Russian coast, the transport model fails to reproduce that feature.

Figure 3 shows three day comparisons between the SeaWiFS-derived dust index images (a, c, and e) and the model-predicted dust concentration (b, d, and f) over the Pacific for days April 19-20, 22-23, 25-26, 1998. A major dust event occurred in desert area of China on April 15 and the generated dust airmass was transported over the Pacific to be observed in California. By comparing these images, the core part of the dust airmass shown in the model concentration is not reflected in the satellite imageries although they well depict low to middle dust concentration area.

CONCLUSION

In comparison with the model-predicted dust concentration field, the dust index imagery reveals fine feature of airmass (see Fig. 2 (a) and (b)). This is obviously because of the difference in spatial scale: While the model calculation was conducted with grid spacing of 120 km or 200 km, the dust index was calculated for each pixel with 4*4 km sampling. Another essential difference is that since the current dust index is only calculated for "clear" pixels whose $\rho_A(865)$ is less than 10%, thick aerosol pixels are automatically masked and excluded. If we are more interested in evaluating the dust mass transport, our dust index algorithm should be extended so that it can work over highly reflective area.

In terms of ocean color atmospheric correction, however, we should secure better sensitivity in detecting thin dust aerosol. Moreover, the dust index should be quantitative enough because "dust correction" scheme apparently requires correct evaluation of relevant parameters such as volume mixture ratio of dust to the total. To develop such a quantitative algorithm, intensive radiative transfer simulation experiments should be conducted. This, of course, requires reasonable modeling on the optical properties of dust airmass.

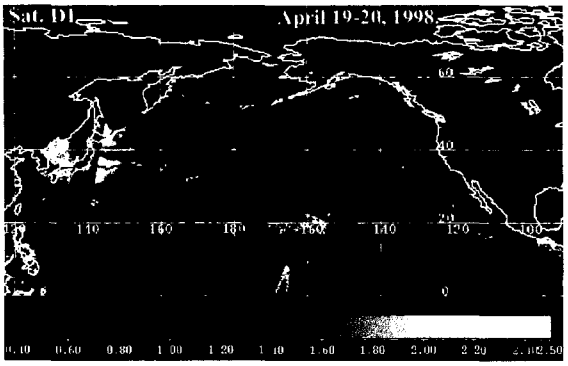

(a)

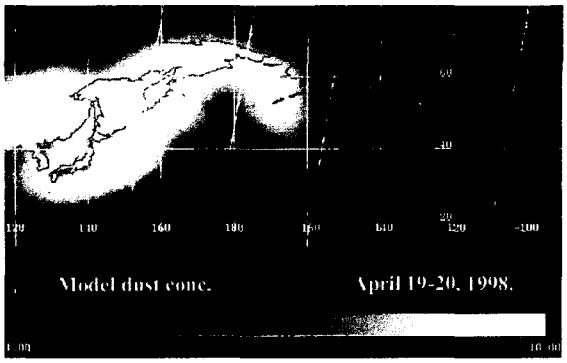

(b)

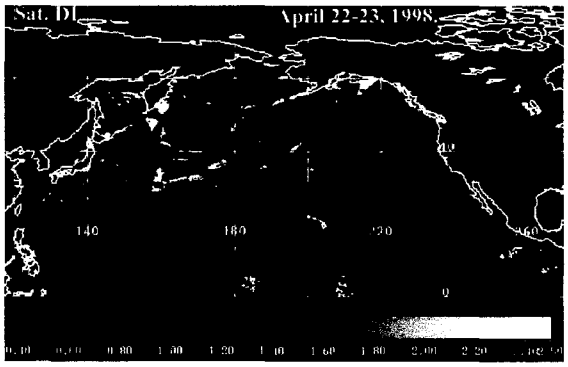

(c)

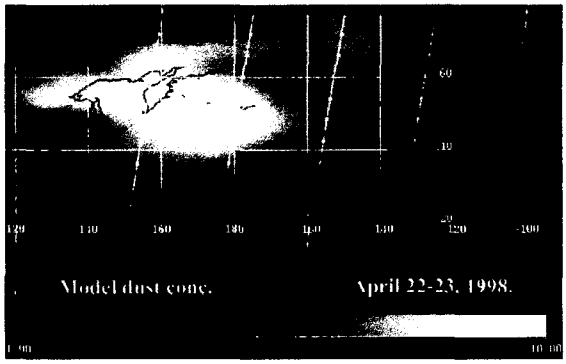

(d)

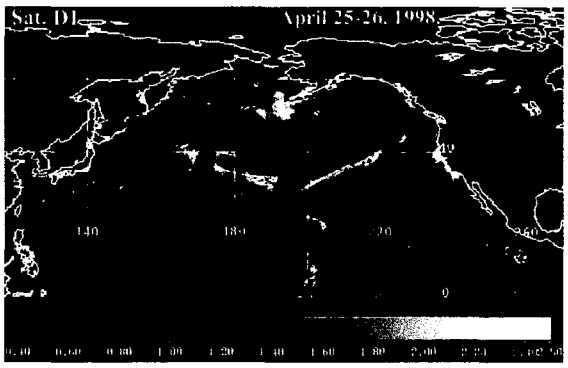

(e)

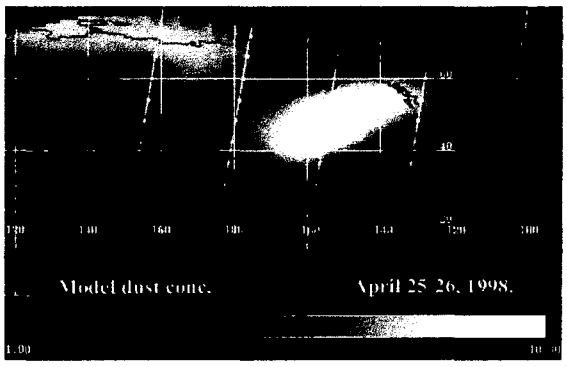

(f)

Figure 3. Three day comparisons between the satellite-derived dust index imagery (a, c, and e) and the model-predicted average dust concentration (b, d, and e), for days April 19-20 (a and b), 22-23 (c and d), and 25-26 (e and f), 1998 over the Pacific. A major dust airmass was formed in Chinese main land on April 15 and transported over the Pacific to reach the U.S. west coast. The original model average dust concentration data were calculated for every 3 hours and time-interpolated with respect to the SeaWiFS observation time. The interpolated dust concentration data for each SeaWiFS orbit were overlayed to form the composite images (b), (d), and (f).

ACKNOWLEDGEMENTS

The authors are grateful to the SeaWiFS/SIMBIOS project at NASA Goddard Space Flight Center for providing supports to conduct this study. We specially thank to B. Franz and W. Robinson for their help and discussion.

This work was in part supported by the Japan-Korea Basic Scientific Promotion Program sponsored jointly by Japan Society for the Promotion of Sciences (JSPS) and Korea Science and Engineering foundation (KOSEF), and by National Space Development Agency of Japan (NASDA) under contract.

REFERENCES

Fukushima, H., and M. Toratani, Asian dust aerosol: optical effect on satellite ocean color signal and a scheme of its correction, *J. Geophys. Res.*, **102** (D14), 17,119-17,130 (1997)

Gordon, H. R., Atmospheric correction of ocean color imagery in the Earth observing system era, *J. Geophys. Res.*, **102**, D14, 17,081-17,106 (1997)

Herman J. R., P. K. Bhartia, O. Torres, C. Hsu, C. Seftor, E. Celarier, Global distribution of UV-absorbing aerosols from Nimbus 7/TOMS data, *J. Geophys. Res.*, **102**, D14, 16911-16922 (1997)

Maritorena, S., J. E. O'Reilly, and B. D. Schieber, The Sea BAM evaluation data set, The SIMBIOS Project.

Moulin C., F. Guillard, F. Dulac, and C. E. Lambert, Long-term daily monitoring of Saharan dust load over ocean using Meteosat ISCCP-B2 data 1: Methodology and preliminary results for 1983-1994 in the Mediterranean, *J.* Geophys. Res., **102**, D14, 16947-16958 (1997a)

Moulin C., F. Dulac, C. E. Lambert, P. Chatenet, I. Jankowiak, B. Chatenet, and F. Lavenu, Long-term daily monitoring of Saharan dust load over ocean using Meteosat ISCCP-B2 data 2: Accuracy of the method and validation using Sun photometer measurements *J. Geophys. Res.*, **102**, D14, 16959-16969 (1997b)

O'Reilly, J. E., S. Maritorena, B. G. Mitchell, D. A. Siegel, K. L. Carder, S. A. Garver, M. Kahru, and C. McClain, Ocean color chlorophyll algorithms for SeaWIFS, *J. Geophys. Res.*, **103**, C11, 24,937-24,953, (1998)

Uno, I., Numerical modeling of trans-Pacific yellow sand (KOSA) transport observed in April, 1998, Presentation at Workshop on Mineral Dust June 9-11, Boulder, CO., http://www.riam.kyusyu-u.ac.jp/taikai/labs/new.html, (1999)